Mon. Not. R. astr. Soc., (1986) **218,** 363–384

Infrared spectropolarimetry of the Galactic Centre: magnetic alignment in the discrete sources

David K. Aitken★, Patrick F. Roche†, Jeremy A. Bailey†, Gordon P. Briggs★, James H. Hough‡ and John A. Thomas★

★ *Department of Physics (RAAF Academy), University of Melbourne, Parkville, Victoria 3052, Australia*

† *Anglo–Australian Observatory, PO Box 296, Epping, N8W 32121, Australia*

‡ *Physics Department, Hatfield Polytechnic, Hatfield, Hertfordshire AL10 9AB*

Accepted 1985 August 16. Received 1985 July 29; in original form 1985 April 22

Summary. We present the results of 8–13 μm spectropolarimetric observations of Galactic Centre sources. All the sources show interstellar polarization due to absorption by aligned silicate grains and these grains appear to be spatially separated along the line-of-sight from those which produce the polarization at shorter wavelengths. The line of sources IRS 1, 10, 5 and 8 comprising the northern arc all show strong intrinsic polarization due to thermal emission from aligned grains of amorphous silicate-like material. This polarization is very uniform among these sources with position angle closely normal to the line of the arc. It is shown that the data are inconsistent with grain alignment due to streaming, but favour alignment by a strong magnetic field >10 mG directed along and linking the northern arc of sources. A field of this magnitude will have significant influence on the structure and evolution of sources in the Galactic Centre, and some possible implications are discussed.

1 Introduction

Infrared polarization in the Galactic Centre was first reported by Dyck, Capps & Beichman (1974) and later studies (Capps & Knacke 1976) showed a polarization peak near 10 μm characteristic of dichroic absorption by aligned silicate grains. Subsequent polarimetry at 2.2, 3.5 and 11.5 μm of some of the discrete sources (Knacke & Capps 1977, KC) showed a roughly uniform polarization of the 2.2-μm sources with position angle close to the Galactic plane, a result confirmed over a wider field by Kobayashi *et al.* (1980), but that at 11.5 μm the position angle of the polarization varies between sources and with a tendency to be orthogonal to the Galactic plane. KC considered that at short wavelengths absorption by aligned grains in the interstellar medium produces the polarization but that at longer wavelengths some mechanism

intrinsic to the individual sources is operating; they favoured absorption by magnetically aligned grains close to these sources. Further broad-band polarimetry at 1.6, 2.2 and 3.5 μm was obtained by Lebofsky *et al.* (1982, LRDK), who argued that the intrinsic component was due to thermal emission from aligned grains in the 10-μm sources. Magnetic alignment by the Davis–Greenstein mechanism (Davis & Greenstein 1951, DG) is discounted by these authors, on account of the large ~10 mG fields required in these dense regions, in favour of alignment by streaming of grains through gas (Gold 1952; Purcell 1969a). Here radiation pressure from stars, which Lebofsky and collaborators consider are embedded in the 10-μm sources, is supposed to drive the streaming. The polarization through the infrared is pictured as a mixture of unpolarized starlight, dominant at H and K, and intrinsic emission which contributes at L and beyond, all subject to the interstellar polarization.

However, Bailey, Hough & Axon (1984) have pointed out that the variation of position angle with wavelength from H, K, L to 11.5 μm appears to be inconsistent with this picture. They consider that intrinsic emission from aligned grains contributes at wavelengths as short as 2 μm with different clouds contributing to the radiation at different wavelengths.

If grain alignment is due to streaming, net polarization can only arise if the dust is anisotropically distributed about the sources, as Lebofsky and collaborators have pointed out. It is then difficult to see how the very similar and large polarization and the apparent correlation of position angle with the direction of the arc of sources IRS 2–1–10–5 shown by the results of KC could arise in this way.

In order to separate the roles of interstellar and intrinsic polarization and clarify the nature of the intrinsic mechanism we have undertaken spectropolarimetric studies between 8 and 13 μm of 10 regions in the central region of the Galaxy.

2 Observations

The observations were made in 1983 August and 1984 May using the $f/36$ focus of the AAT with the UCL cooled grating array spectrometer as modified for spectropolarimetry. The observing procedures are similar to those described in Aitken *et al.* (1984, 1985) and a 4.2-arcsec aperture with 50-arcsec NS beam throw was used for all the measurements. Corrections for telluric absorption and intensity calibration were from observations of η Sgr at similar airmasses. η Sgr has a small excess in the 8–13 μm region compared with main-sequence A stars; the intensity spectra have been corrected for this by reference to observations of α CMa made on the same night. The polarization fractions and position angles are unaffected by telluric and instrumental transmission, since they are derived from ratios of the Stokes parameters; their errors are affected, however. The position angle calibration was from the Becklin–Neugebauer source (BN) in Orion taking this to be 118° as found by Capps and by ourselves in a separate calibration using the IRTF (Aitken *et al.* 1985). The instrumental polarization was found to be <0.25 per cent from observations of α CMa and η Sgr.

Observations were made of 10 regions in SgrA with a spectral resolution $\Delta\lambda = 0.23\,\mu$m at a single grating setting, sampling the 25 wavelength channels simultaneously. Higher resolution studies with $\Delta\lambda = 0.025\,\mu$m were also made of two of the sources around the wavelength of the Ne II emission line at 12.81 μm. Offsets were made from IRS 3 because at 10 μm it is unresolved and sufficiently well separated from its neighbours; Table 1 gives a log of observations together with these position offsets. As we have noted before, because of the exigencies of spectropolarimetric work the quality of the spectra must be very good. Even the low-resolution observations yield intensities and equivalent widths of the [Ne II] fine structure line; these are confirmed in two sources (1, 10) for which higher resolution studies were made. These results are listed in Table 2, and the spectra shown in Fig. 1(a). In describing the sources, we use the

Table 1. Log of observations.

Source	Offset from IRS 3 (arcsec)		Date	Notes
IRS 1	8.5 E	3.5 S	1983 August 20	1
			1984 May 11	2
IRS 2	1.5 W	8.5 S	1983 August 20	1
IRS 3	–	–	1983 August 20	1
IRS 4	16.0 E	9.5 S	1983 August 20	1
IRS 5	11.3 E	4.5 N	1984 May 12	1
IRS 6	5.5 W	2.0 S	1983 August 20	1
IRS 8	5.5 E	26.5 N	1983 August 21	1
IRS 9	6.5 E	10.5 S	1984 May 11	1
IRS 10	9.5 E	1.0 N	1983 August 20	1
			1984 May 11	2
'Ridge'	2.0 E	8.0 S	1984 May 11	1

1. 7.7–13.3 μm at $\Delta\lambda=0.23\mu$m.
2. 10.8–12.5μm at $\Delta\lambda=0.09\mu$m and 12.75–12.86μm at $\Delta\lambda=0.03\mu$m.
All observations with 4.2 arcsec aperture and 50 arcsec throw N–S.

nomenclature of Becklin *et al*(1978) and the positions of the individual sources are indicated in Fig. 6.

There is a wide range of intensity between the sources and through each spectrum, and the polarization signal/noise ratio is often poor in the silicate minimum, which is also affected by telluric absorption, and the region shortward of ~8.5μm, where the waveplate efficiency is falling. To improve the signal/noise ratio the Stokes parameters have been averaged over two wavelength channels in presenting the polarization data, except near the Ne II line in IRS 1; the effective bandpass is then indicated by the spacing between points (Fig. 1). Because polarization is a positive definite quantity, errors of measurement tend to introduce a positive bias. We use the following prescription (Wardle & Kronberg 1974) to reduce this tendency:

$$P^2=Q^2-dQ^2+U^2-dU^2$$

Table 2. Spectral data.

	Silicate ratio (see text)	$T_{\rm eff}$ (K)	Ne II line Intensity (10^{-18} W cm^{-2})	Equivalent width (μm)	Continuum at 12.8μm (10^{-17} W cm^{-2} μm^{-1})
IRS 1	0.88±0.03	198±20	7.1±0.5	0.022±0.002	35.0
			6.6±0.2	0.021±0.001	30.5★
IRS 2	0.72±0.03	173±10	9.0±0.5	0.066±0.004	15.0
IRS 3	–	–	0.9±0.2	0.007±0.002	14.8
IRS 4	0.54±0.03	140±5	3.8±0.5	0.060±0.008	6.9
IRS 5	0.71±0.03	157±8	4.1±0.5	0.041±0.005	10.0
IRS 6	0.07±0.03	152±7	3.8±0.5	0.042±0.005	10.0
IRS 8	0.24±0.03	190±12	2.2±0.5	0.038±0.009	5.7
IRS 9	0.62±0.02	165±10	2.5±0.5	0.029±0.006	8.3
IRS 10	0.74±0.02	170±12	3.9±0.5	0.021±0.003	20.5
			3.7±0.2	0.020±0.001	18.0★
'Ridge'	0.78±0.03	165±12	8.1±0.5	0.056±0.003	15.5

★High resolution.

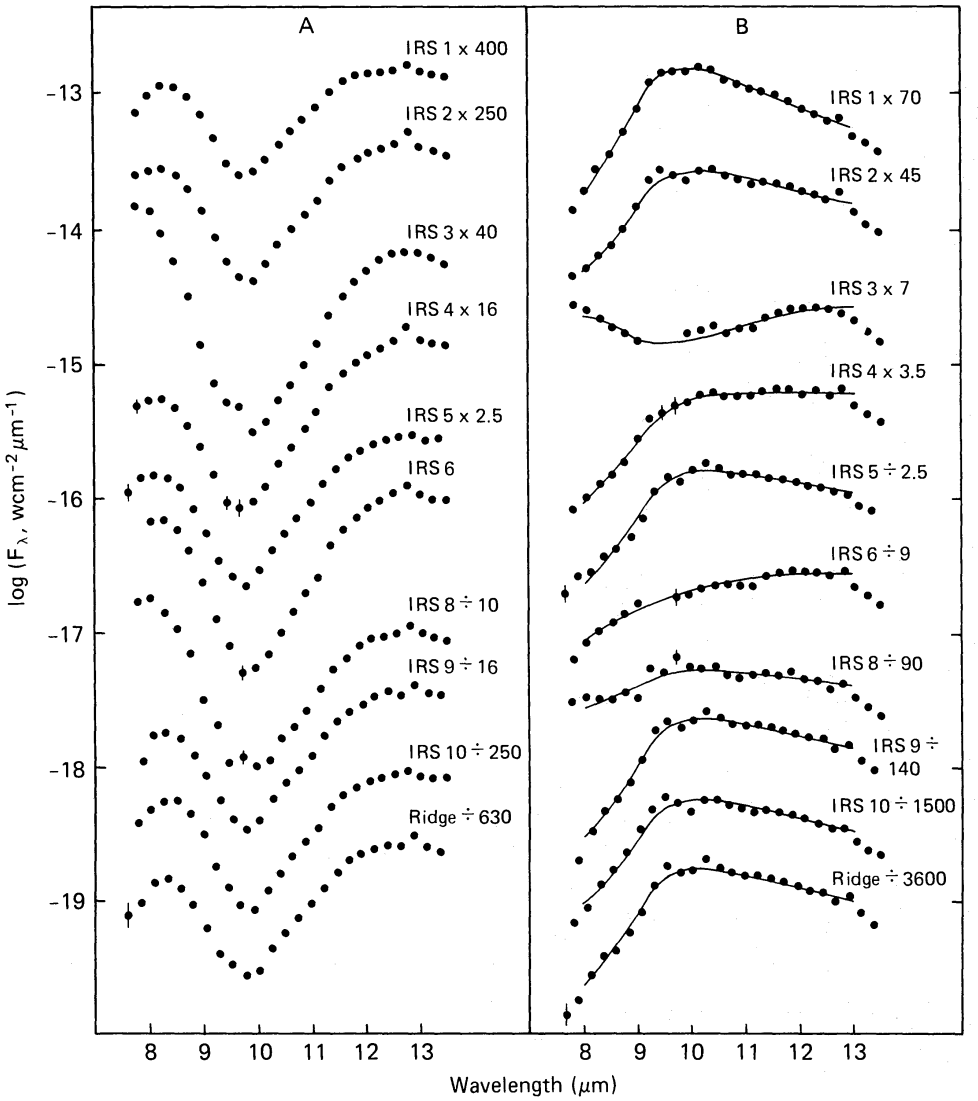

Figure 1. (a) Observed 7.7–13.3μm spectra of Galactic Centre sources, and (b) after dereddening with a μCep emissivity curve of peak optical depth $\tau_{\mu\,\mathrm{Cep}}$=3.6 (see text). Solid lines show best fits to a mixture of μCep and smooth emissivity (see text). Errors are shown when they exceed 4 per cent of the signal.

where Q and U are the usual Stokes parameters. P is set to zero if the RHS is negative and the position angle is considered undetermined.

3 Results and discussion

3.1 THE SPECTRA

As has become well known, all the mid-infrared sources within the central arcminute of the galaxy show similar strong absorption near 9.7μm. The spectra of 10 of these sources are shown in Fig. 1(a); some of these have already been published (Roche & Aitken 1985, RA). The absorption feature is narrower than that seen towards dense molecular clouds and is similar to the absorption in the interstellar medium (Roche & Aitken 1984). It is better represented by the emissivity observed in an oxygen-rich circumstellar shell (μ Cep, Russell, Soifer & Forrest 1975) rather than that of the Trapezium which usually provides a good fit to the molecular cloud sources. The ratio

$A_V/\tau_{9.7}$ is distinctly smaller than found for the local interstellar medium and RA argue that this is likely to be due to an excess of oxygen-rich grains in the inner regions of the Galaxy, consistent with the observed deficiency of carbon stars in the Galactic Bulge (Blanco, Blanco & McCarthy 1978).

It is generally agreed that, with the possible exception of IRS 3, all the sources studied here lie within a parsec of the dynamical centre of the Galaxy, and similar interstellar extinctions are expected to all of them. In fact silicate absorption of a mixture of greybody plus optically thin silicate emission gives tolerable best fits with a very similar absorption depth of $\tau_{\mu\ \mathrm{Cep}}=3.6\pm0.3$ for all the sources except IRS 3 for which $\tau_{\mu\ \mathrm{Cep}}\simeq4.4$, probably implying local obscuration of this source. As noted in RA, when the sources are dereddened by $\tau_{\mu\ \mathrm{Cep}}=3.6$ they vary significantly in the form of their underlying emission, with IRS 1 displaying the most prominent silicate emission feature.

A quantifiable measure of the relative strength of silicate emission is obtained by fitting the dereddened spectra using a mixture of μ Cep-like emissivity for the silicate and a λ^{-2} emissivity for the smooth component; the temperatures of these components are constrained to equality to avoid divergence of the μ Cep temperature. Although equality of the temperatures is unlikely in practice, the temperature obtained can be regarded as an effective source temperature, T_{eff}, for the grains which radiate at 10μm. For example in IRS 1, where the especially strong silicate emission allows the silicate temperature to be left free, the temperatures of both components agree to within 15 K. Use of a grey emissivity rather than the λ^{-2} wavelength dependence gives slightly poorer fits and raises T_{eff} by about 40 K. The dereddened spectra and fits are shown in Fig. 1(b); Table 2 lists the μ Cep/total emissivity ratios and effective temperatures, the observed [Ne II] intensities and equivalent widths and the 12.8–μm continuum level. T_{eff} is in the range 150–200 K for most of the sources and would be 200–250 K if the smooth component were grey. It is noticeable that the [Ne II] emission from the IRS 3 position is much weaker than from the other sources, and in view of the beam size and throw used it is likely that this neon emission is diffuse and unrelated to IRS 3. There is no sign of IRS 3 in the radio structure (Lo & Claussen 1983; Brown & Liszt 1984) and it seems that IRS 3 is not an ionized region, further distinguishing it from the other 10-μm sources. Note also that the Ne II line intensity increases from IRS 1 through 'Ridge' to IRS 2, a result which echoes the radio distribution, while the strongest 10-μm continuum source is IRS 1.

3.2 THE POLARIZATION

Fig. 2(a–j) gives the polarization percentages and position angles from 7.7 to 13.3μm for the sources in Fig. 1. Table 3 compares the 11.5μm broadband results of KC in a 7-arcsec beam and of Capps & Knacke (1976) in an 11-arcsec beam with equivalent quantities derived from the present data for the wavelength range 10.85–12.15μm. For many of the sources the agreement is satisfactory (IRS 1, 3, 4, 10) notwithstanding the difference in beam size, while in others (2, 5, 8, 9) there appear to be significant discrepancies, especially in position angle. Since in this wavelength interval all the sources have large variations in intensity and some have rapid changes of polarization parameters it may be that different weighting in the interval accounts for some of the discrepancies, while part may simply be due to beam size effects.

The polarization properties divide the sample into two categories: first, those that show a polarization peak of 4–8 per cent near 10μm with only small polarization near 13μm (3, 4, 6, 9) and, secondly, those in which a 10-μm peak is not prominent but have polarizations increasing to 4–6 per cent at 13μm (1, 5, 8, 10). Sources 2 and 'Ridge' have a blend of these characteristics. Most of the sources show changes of polarization position angle through the spectrum which suggests that more than one polarization mechanism is at work; however IRS 3 shows little

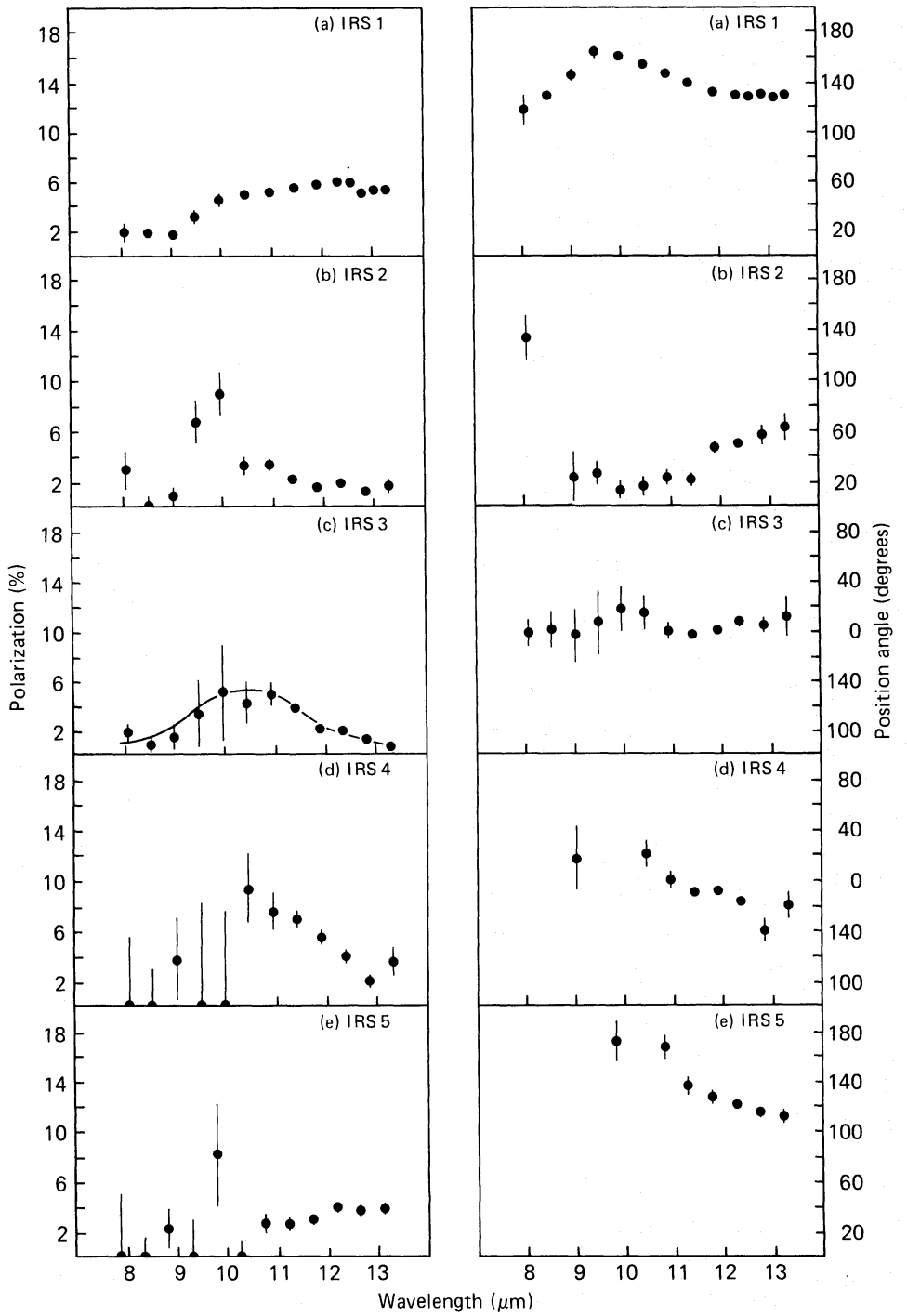

Figure 2. Observed polarization percentage and position angle for the sources shown in Fig. 1. Errors are shown when they exceed 0.3 per cent in polarization and 4° in position angle. The solid line in (c) is the polarization curve towards the BN object scaled to the IRS 3 data (see text).

position angle change with wavelength. In IRS 1 there is a reduction in polarization in the [Ne II] line, which is confirmed by the high-resolution observations (Fig. 3). The effect is also present in IRS 10 and there is a position angle change in both sources. We can separate the line and continuum polarizations by subtraction of the relevant Stokes parameters and in this way find the polarization in the [Ne II] line to be 2.9 ± 0.9 per cent at position angle $0 \pm 9°$. Since scattering at

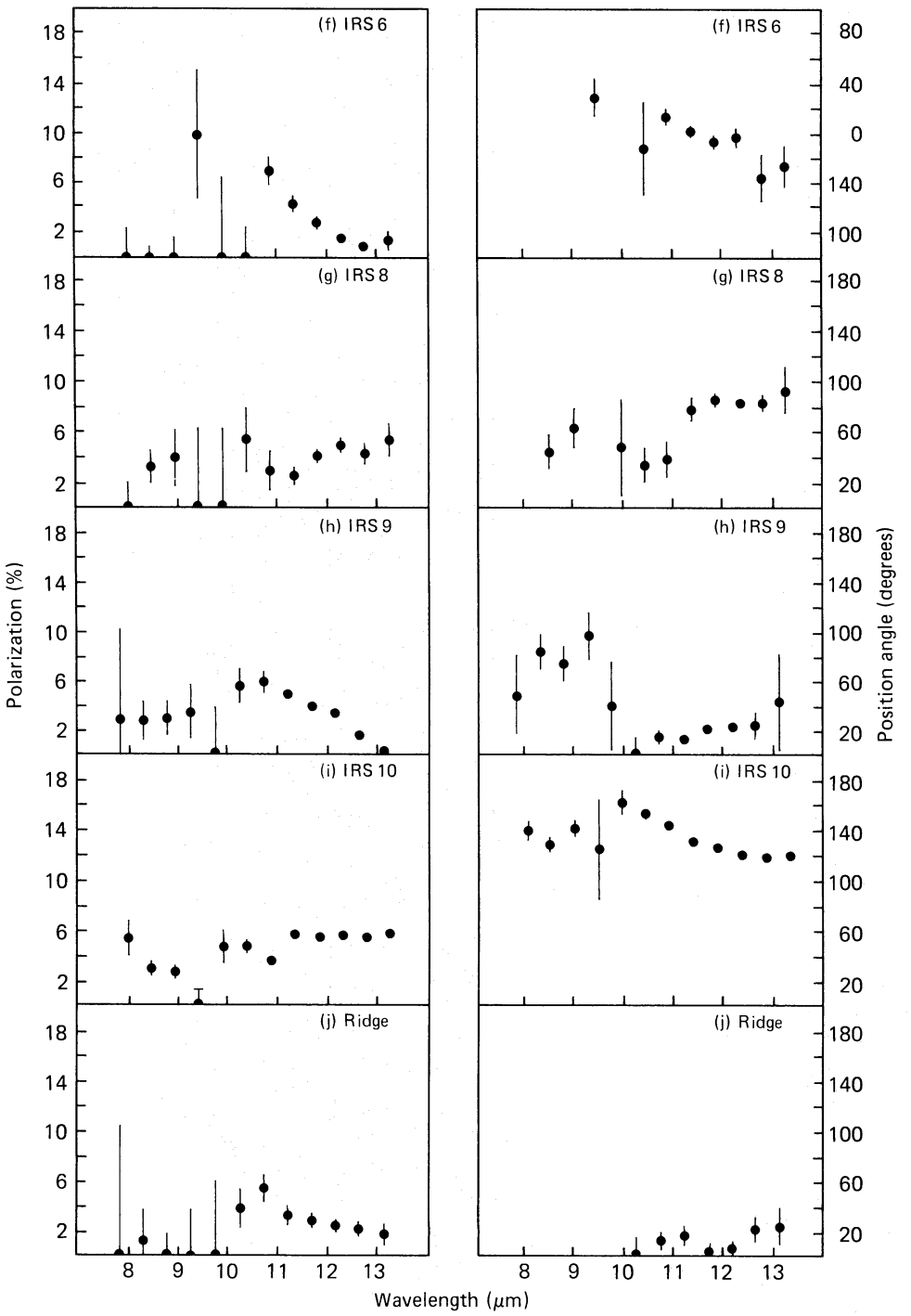

Figure 2 – *continued*

these wavelengths is likely to be insignificant we regard the neon line as having no intrinsic polarization so that its polarization represents that of the interstellar medium at 12.8μm. Removing this interstellar component we find the intrinsic polarization of the continuum emission from IRS 1 at this wavelength to be 7.6±0.9 per cent at 113±4°.

Because all the sources suffer similar extinctions by the material along the line-of-sight and the polarizations and position angles of the sources at 2.2μm are all similar, we expect similar interstellar polarizations at 10μm. We therefore ascribe the changing polarizations and position

Table 3. Broad-band polarization percentage and position angle (degrees).

	11.5μm		10.85–12.15μm (this work)		12–13μm intrinsic (see text)	
	p	θ	p	θ	p	θ
IRS 1	5.9±0.5	139±5 (1)	5.5±0.6	133±4	6.5±0.6	119±4
	4.0±0.3	134±8 (2)			(7.6±0.9	113±4) (3)
IRS 2	3.5±0.6	173±6 (1)	1.9±0.8	33±11	2.9±0.6	76±6
IRS 3	4.1±0.8	170±6 (1)	3.0±0.5	179±5	0.6±0.5	61±20
	3.8±0.9	153±12 (2)				
IRS 4	4.7±0.9	168±10 (2)	6.4±0.3	172±3	2.1±0.4	137±5
IRS 5	2.4±0.4	100±5 (1)	3.2±0.3	131±3	5.3±0.4	107±3
	2.7±0.5	82±10 (2)				
IRS 6			4.0±0.7	178±5	1.1±0.4	103±11
IRS 8	6.6±1.7	106±7 (1)	3.4±0.5	77±4	6.8±0.5	84±2
IRS 9	5.2±0.5	173±5 (1)	4.7±0.5	17±3	1.6±0.4	54±8
IRS 10	4.7±0.4	129±5 (1)	5.3±0.7	130±4	6.9±0.6	113±3
'Ridge'			3.1±0.5	9±5	1.6±0.5	48±9

1. Knacke & Capps (1977), 7-arcsec beam.
2. Capps & Knacke (1976), 11-arcsec beam.
3. Evaluated at 12.8μm assuming that the [Ne II] line is not intrinsically polarized (see text).

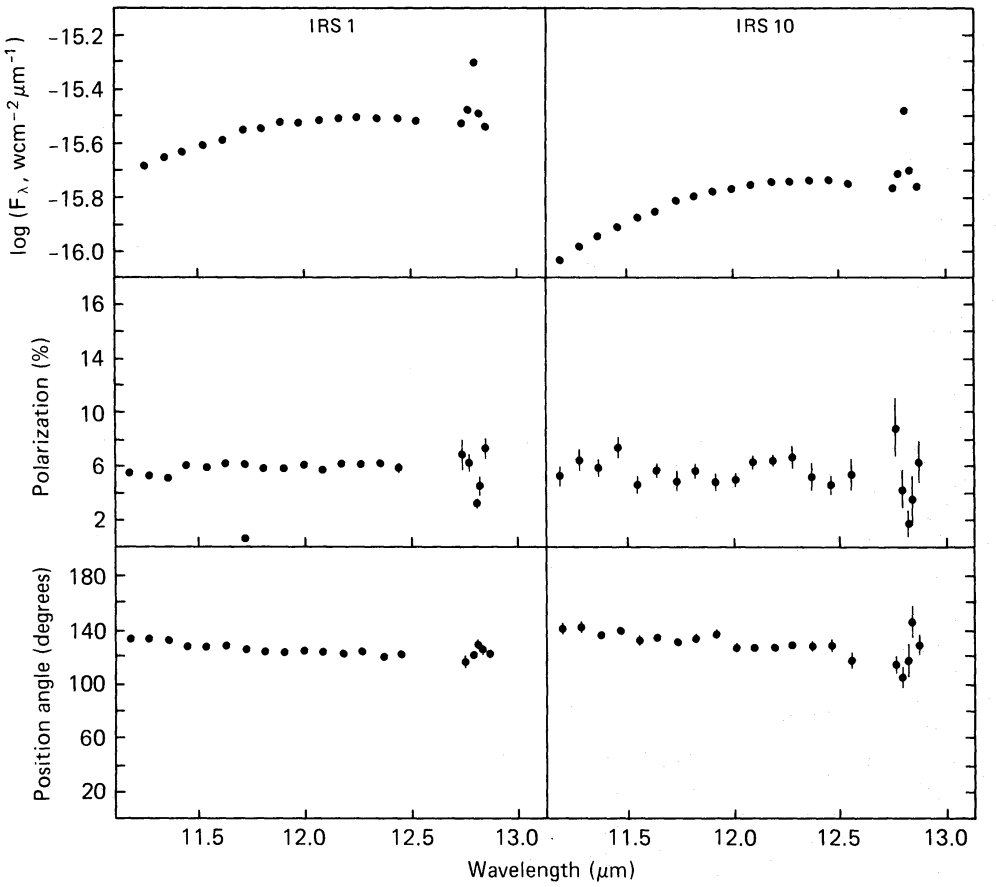

Figure 3. Intensity, polarization percentage and position angle for IRS 1 and 10 at higher spectral resolution showing the [Ne II] line at 12.81μm.

angles to intrinsic polarization in each of the sources. This intrinsic polarization appears to be stronger in the arc sources 1, 5, 8, 10 and the large polarization at long wavelengths strongly suggests thermal emission from aligned grains since, in emission, grains give a polarization fraction nearly independent of optical depth (e.g. Martin 1975, also Section 3.4.1 in this work). This is further evidence in favour of the suggestion of LRDK, based on the range of position angles at 10 μm compared with 2.2 μm and the small optical depth of the 10-μm sources, that the mid-infrared polarization has a component due to thermal emission from aligned grains. For aligned silicate grains in particular, the emission polarization will be larger at long wavelengths because the polarized intensity peaks at longer wavelengths than does the emissivity (e.g. Martin 1975; Hong & Greenberg 1978).

3.3 THE INTERSTELLAR COMPONENT OF POLARIZATION

Many of the sources (3, 4, 6, 9) show a polarization spectrum similar to that of the BN object in Orion (e.g. Dycke & Lonsdale 1981, and references therein; also Aitken *et al.* 1985, (ABRH), and in IRS 3 the change in position angle with wavelength is small. There is little doubt that the polarization at 10 μm in Orion is due to dichroic absorption by aligned silicate grains, although the alignment mechanism, there and elsewhere, has been the subject of discussion (e.g. ABRH and references therein). Similar polarization spectra are found to be common in heavily obscured infrared sources (Dycke & Lonsdale 1981; Heckert & Zeilik 1984; our work in preparation), and it is clear that alignment of dust grains in the interstellar medium and molecular clouds is the rule rather than the exception.

Martin (1975) has shown that the form of $P(\lambda)/\tau(\lambda)$ is related to the band strength of the grain material. In Fig. 4 we show $P_{\mathrm{IRS\,3}}(\lambda)/\tau_{\mathrm{IRS\,3}}(\lambda)$ and $P_{\mathrm{BN}}(\lambda)/\tau_{\mathrm{BN}}(\lambda)$, where $\tau_{\mathrm{IRS\,3}}(\lambda)$ is the μ Cep emissivity scaled to 3.6 and $\tau_{\mathrm{BN}}(\lambda)$ is the Trapezium emissivity scaled to 3.3 at 9.7 μm; the comparison suggests polarization of similar kind in both sources showing that the line-of-sight material to the Galactic Centre has similar band strength to that of molecular cloud material, notwithstanding the different shape of the absorption feature. The average alignment along this line-of-sight is about half that towards BN in Orion, if similar grain shapes are involved.

Since all the sources here are subject to essentially the same extinction and short wavelength polarization we investigate the effect of a suitably scaled absorptive polarization, $P_{\mathrm{BN}}(\lambda)$, having similar wavelength dependence to BN, being present in all the sources. We have noted above,

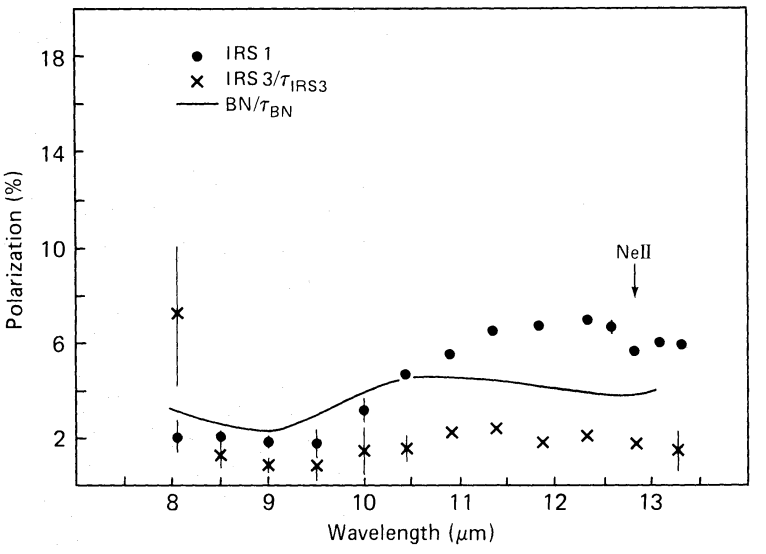

Figure 4. Comparison of the intrinsic polarization in IRs 1 (see text) with p/τ for IRS 3 and the BN object.

and in RA, that the extinction to the Galactic Centre contains a larger proportion of silicate material than the local interstellar medium, and we consequently expect less polarization near 8 μm relative to 10 μm than provided by the BN curve. To allow for this we have subtracted a λ^{-2} component from $P_{\rm BN}(\lambda)$ to reduce the 8 μm polarization to small values. This modification is small but does improve slightly the representation of the interstellar component of polarization.

We therefore treat the interstellar medium in the line-of-sight to the Galactic Centre as an imperfect polarizer of efficiency $P_{\rm IS}(\lambda)=\alpha\{P_{\rm BN}(\lambda)-\beta\lambda^{-2}\}$ orientated at a position angle ϕ, where β is adjusted to make $P_{\rm IS}(\lambda)\simeq 0$ at 8 μm. Then if I', Q', U', V' and I, Q, U, V are the observed and intrinsic Stokes parameters of each source,

$$\begin{bmatrix} I' \\ Q' \\ U' \\ V' \end{bmatrix} = \exp(-\tau) \begin{bmatrix} 1 & P\cos 2\phi & P\sin 2\phi & 0 \\ P\cos 2\phi & 1-P\sin^2 2\phi & P\cos 2\phi\,\sin 2\phi & 0 \\ P\sin 2\phi & P\cos 2\phi\,\sin 2\phi & 1-P\cos^2 2\phi & 0 \\ 0 & 0 & 0 & 1-P \end{bmatrix} \begin{bmatrix} I \\ Q \\ U \\ V \end{bmatrix}$$

(e.g. Serkowski 1962), where $\tau(\lambda)$ is the optical depth averaged over orthogonal polarization position angles, and for brevity $P=P_{\rm IS}(\lambda)$. From IRS 3 we see that P should take on a peak value $P_{\rm m}\simeq 5$ per cent in the 8–13 μm region and that the nearly constant position angle is $0\pm 5°$, agreeing with $0\pm 9°$ derived from the neon-line polarization, and thereby supporting our earlier assumption that the [Ne II] line is intrinsically unpolarized. By simple matrix inversion we find the Stokes parameters of the intrinsic emission, and since here we are interested only in polarization and position angle can drop the $\exp(-\tau)$ factor; the deconvolved intrinsic polarizations found are shown in Fig. 5(a–j).

In this way the intrinsic polarization of IRS 3 is found to be essentially zero over the wavelength range, which again demonstrates the close similarity of the IRS 3 and BN polarization spectra; IRS 6 also shows no significant intrinsic polarization. When the procedure is applied to IRS 1, it produces a position angle almost independent of wavelength, and in most of the other sources there is a reduction in position angle variation after removal of the interstellar medium polarization.

The 2.2 μm polarization position angle of the whole region is $\simeq 20°$ (Kobayashi *et al.* 1983), significantly different from the value adopted here for the 10 μm region. Using $\phi=20°$ gives poorer cancellation of polarization in IRS 3 and 6 and there is more variation of position angle in IRS 1. In all other sources here the position angle variation is less for $\phi=0°$ rather than $\phi\simeq 20°$. We conclude that there is a real position angle difference between the 2 and 10 μm interstellar polarization.

A rotation of the polarization plane with wavelength is possible if there is a change of alignment angle and grain composition along the line-of-sight. The line-of-sight to the Galactic Centre passes through several spiral arms, and it has already been suggested (RA) that the innermost regions contain an excess of silicate material, to account for the low ratio $A_V/\tau_{\rm sil}$ compared with that found for the local interstellar medium. Note also that the 2.2 and 10 μm polarizations are comparable and $\sim$5 per cent (KC, LRDK, and Kobayashi *et al.* 1983) whereas in the BN object the 2.2 μm polarization is nearly twice that at 10 μm. If, at 2.2 μm, as is thought to be the case in the visible, the extinction is mainly due to a carbon-based component, e.g. the grain model of Lee & Draine (1985), while that at 10 μm is due to silicates, the present discrepancy between position angles and the lower ratio of polarizations at 2.2 and 10 μm add independent support to the suggestion that these components are fractionated along the line-of-sight to the Galactic Centre. Kobayashi *et al.* (1983) have found that there is a change in 2.2 μm polarization position angle for discrete sources within the central 40 arcmin, at a $H-K$ value corresponding to a line of sight

distance of roughly 5 kpc. For $H-K>1.0$ mag the position angle changes from $\sim 170 \pm 10°$ to $\simeq 17°$, which is also the K position angle of the diffuse emission from stars near the Galactic Cente. It appears that there are at least three regions of distinct grain orientation along the line of sight to the Galactic Centre.

With this in mind we could refine the deconvolution procedure by including an additional polarization matrix of featureless material at $\phi = 20°$. If this is done the cancellation of IRS 3 polarization is not as good unless the amount of 10μm polarization produced in this way is very small; there is also no improvement in the position angle variation in the other sources. We conclude that the contribution at 10μm of the material which produces the 2.2μm polarization is negligible. Note also that at 3.5μm the position angle of IRS 3 (KC) is similar to that at 2.2μm for the whole region (the polarization of IRS 3 has not been measured at 2.2μm); hence the same material seems to produce the polarization in the $2–4\mu$m region.

3.4 THE INTRINSIC COMPONENTS OF POLARIZATION

3.4.1 IRS 1

The intrinsic polarization (Fig. 5a) has a weak minimum near 9.5μm and rises steadily to a broad maximum ~ 7 per cent near 12.5μm. Here the interpretation of the polarization spectrum is straightforward on account of the almost complete absence of position angle variation. The data are consistent with emission from grains preferentially aligned in one direction, or if from a variety of orientations, of uniform temperature and composition. If we denote by Q_x and Q_y the averaged absorption efficiency of grains for E-vectors directed along and perpendicular to the projection of the alignment direction on the plane of the sky, then emission from an optically thin ensemble gives a polarization fraction

$$P(\lambda) = -(Q_x - Q_y)/(Q_x + Q_y)$$

(here the polarization is orthogonal to the axis of greatest principal moment of inertia of the grains). Absorption of unpolarized radiation by an optical depth

$$\tau(\lambda) = (\tau_x + \tau_y)/2 = N\pi a^2 (Q_x + Q_y)/2$$

gives polarization

$$P(\lambda) = \tanh\{N\pi a^2 (Q_x - Q_y)/2\} \simeq N\pi a^2 (Q_x - Q_y)/2,$$

and therefore

$$P(\lambda)/\tau(\lambda) \simeq (Q_x - Q_y)/(Q_x + Q_y)$$

provided the difference in optical depths $\tau_x - \tau_y$ is small. Martin (1975) has shown that near a resonance in the dielectric properties of the grain material, the form of $(Q_x - Q_y)/(Q_x + Q_y)$ depends on the band strength and has calculated its wavelength dependence for various idealized silicates. A particular advantage of polarized emission is that it gives $(Q_x - Q_y)/(Q_x + Q_y)$ directly, provided the emission arises from the same population as the polarization, whereas to evaluate this from absorption, as for instance for BN, requires further knowledge of the emissivity through $Q_x + Q_y$. Comparison with the intrinsic polarization in IRS 1 indicates that the emissive grain material in the Galactic Centre has band strength $\sim 4 \times 10^3\,\mathrm{cm}^{-3}$, typical of amorphous silicate materials. The amount of polarization, $\simeq 7$ per cent, implies a fairly strong alignment and large average axial ratio for the emissive grains since perfect spinning alignment in the plane of the sky gives ~ 12 per cent for prolate and ~ 30 per cent for oblate grains of axial ratio 2 (see e.g. Martin 1975; Lee & Draine 1985). $P(\lambda)/\tau(\lambda)$ for BN and IRS 3 are shown in Fig. 4 and compared with the

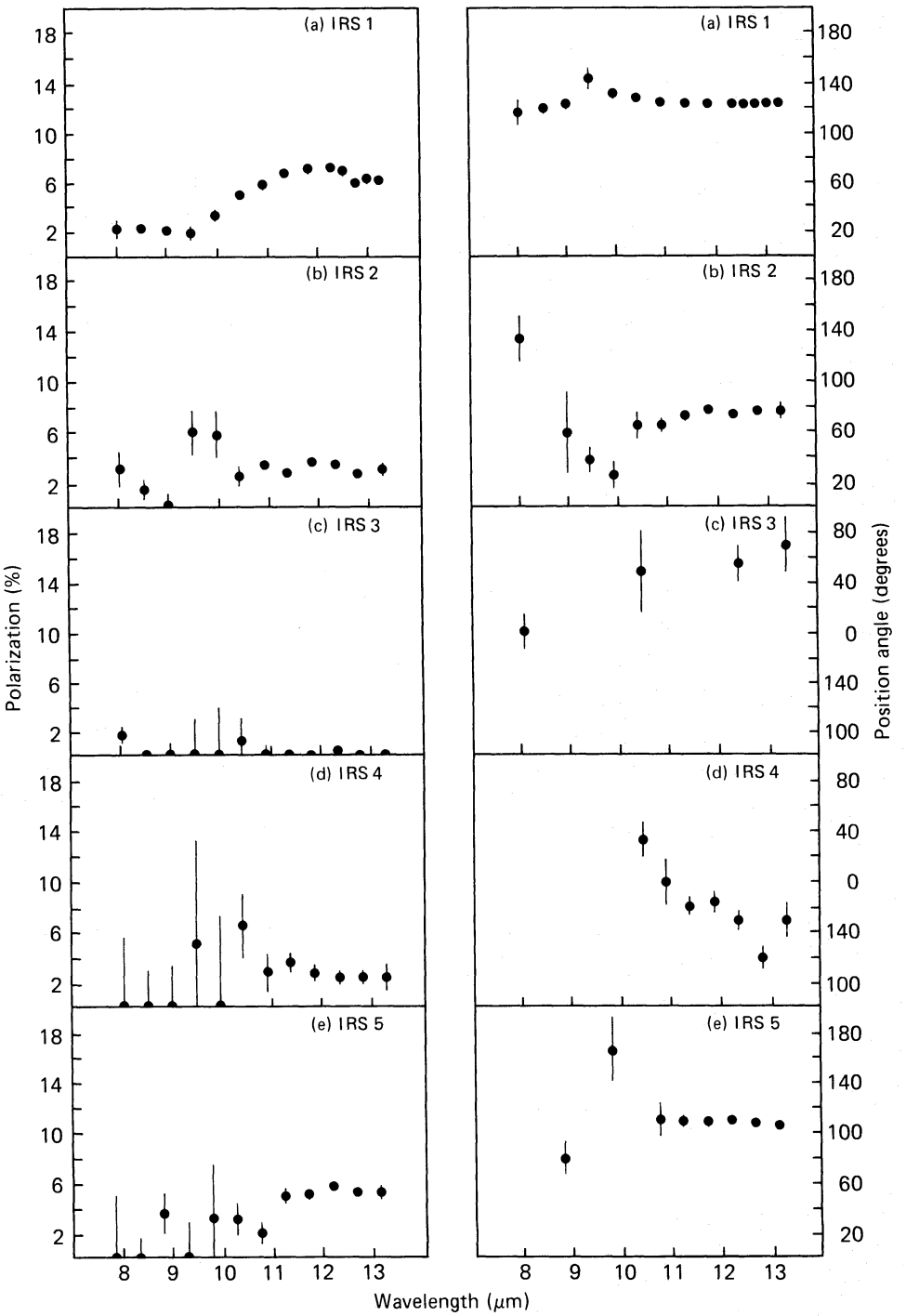

Figure 5. Intrinsic polarization and position angle (see text) for the sources shown in Figs 1 and 2. Other details as in Fig. 2.

intrinsic polarization of IRS 1. It appears that grains are more efficiently aligned in IRS 1 than in Orion along the line-of-sight to BN and by a factor ~3 more than in the interstellar medium to the Galactic Centre. Qualitatively the curves are similar but the quantitative difference suggests that IRS 1 may contain grains with a slightly larger bandstrength than Orion; alternatively the difference may be due to extra emissive components in IRS 1 or BN. It should be borne in mind that we have used (modified) molecular cloud-like material (BN) to deconvolve the interstellar

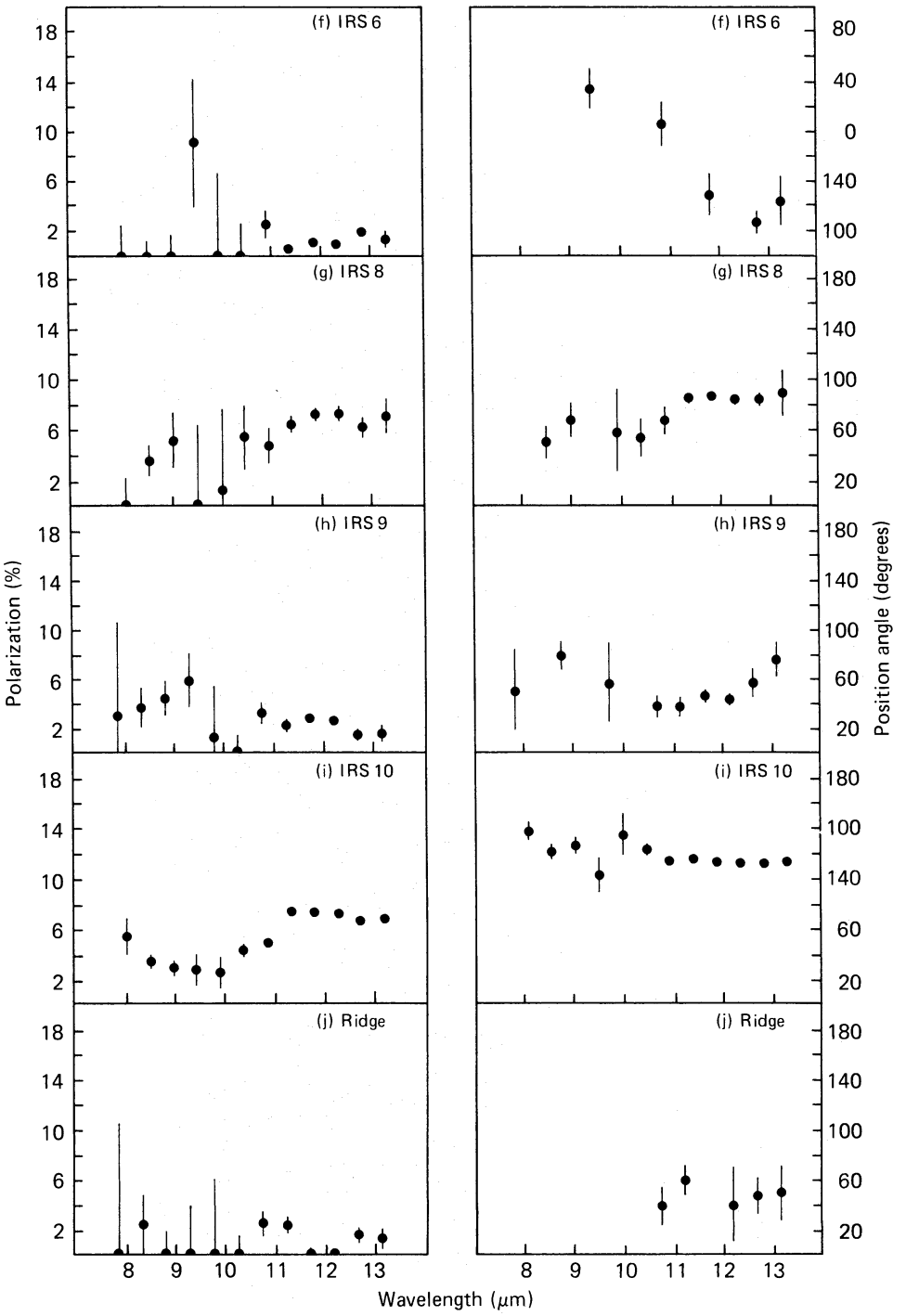

Figure 5 – *continued*

polarization and differences between this and the real properties of the interstellar medium will propagate into the derived intrinsic polarization which we take to be $(Q_x-Q_y)/(Q_x+Q_y)$.

The influence of the interstellar medium will be at least at 8 and 13 μm and the deconvolution subject to smaller errors. Since the data quality is higher at the longer wavelength the intrinsic polarization properties are better determined here, and their values for 12–13 μm in IRS 1 and the other sources are listed in Table 3.

3.4.2 The other sources in the northern arc of emission: IRS 10, 5 and 8

All of these (Fig. 5e, g, i) show polarizations of the same general form and amplitude as IRS 1: an intrinsic polarization increasing towards long wavelengths to a value ≃6–7 per cent near 12.5 μm, and showing little variation in position angle in each source, at least between 10.5–13 μm, where the data quality is good. The same polarization mechanism, thermal emission from aligned silicate-like grains, accounts for the polarization in the arc 1–10–5–8.

3.4.3 The remaining sources: IRS 2, 3, 4, 6, 9 and 'Ridge'

The intrinsic polarization in these sources is much less than in those in the arc. As we have seen, IRS 3 has no detectable emissive component and likewise there is little evidence for such a component in either IRS 6 or the 'Ridge'. However, IRS 2 and 4 show clear emissive components ≃3 and 2 per cent respectively while in IRS 9 there is an indication of a polarization peak near 10 μm and the polarization is still reducing at 13 μm. These sources also show more position angle complexity and the high resolution [Ne II] studies of Lacy and collaborators (Lacy *et al.* 1980, and references to previous work show that these regions have complex velocity structure, implying more than one source in the line-of-sight. The observed position angle variations could be accounted for if these have different alignment directions, provided the grains have different temperatures and/or compositions.

While all the arc sources show polarization between 12 and 13 μm in the range 5.3–7.0 per cent

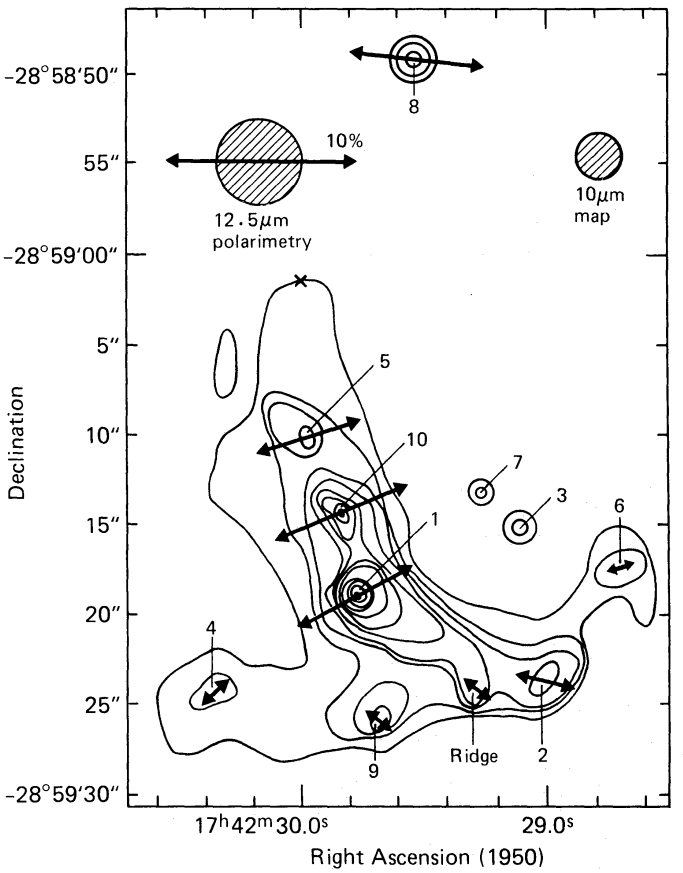

Figure 6. Intrinsic 12.5 μm polarizations (see text) superimposed on the 10 μm map of Becklin *et al.* (1978). Note that the intrinsic polarization of IRS 3 is too small to show on this scale.

and those in the bar have <3 per cent polarization, both groups display a wide range of silicate fraction. Thus there is no evidence for a correlation between silicate emission and polarization, although the observed polarization structure in the arc (Figs 4 and 5) suggests that silicate grains are responsible for the polarization.

Table 3 lists the intrinsic polarization parameters of these sources evaluated between 12 and 13 μm and Fig. 6 shows them plotted on the 10 μm map of SgrA due to Becklin *et al.* (1978). For the arc of sources IRS 1–10–5–8 the polarizations are remarkably large and similar and the *E*-vector is strongly correlated to be normal to the line of the arc. Since in emission, the *E*-vector will be parallel to the long grain dimension, the spin axes of the grains must be directed along the arc. In the other sources the polarization is weaker and the correlation with topographic features less striking, although there is still a tendency for the *E*-vector to be normal to, and therefore the spin axes to be along, the line of sources 4–9–'Ridge'–2.

3.4.4 The 3.5 μm intrinsic polarization

Bailey *et al.* (1984) have pointed out that the observed position angle of IRS 1 at 3.5 μm is inconsistent with an intrinsic polarization at the observed 11.5 μm position angle of 159° (KC) and subject to interstellar polarization with position angle ≈12°; they argued that separate dust clouds must give rise to the intrinsic polarization at these wavelengths. After correction for interstellar absorption the 12–13 μm intrinsic position angle found here is 117°, and almost orthogonal to the adopted near infrared interstellar position angle of 20°, so the situation must be reconsidered. In Table 4 we list the polarization parameters of KC and LRDK and show the effects of removing an interstellar polarization of 3 per cent (roughly half the 2.2 μm polarization, as might be expected at 3.5 μm from an extrapolation of the Wilking *et al.* (1980) formula) at position angle 20°. The intrinsic 3.5 μm polarizations thus found are large for IRS 1, 5, and 10 and essentially zero for IRS 2 and 3. For IRS 9 the removal of interstellar polarization is perhaps incomplete. The derived position angles, which are insensitive to values adopted for the interstellar medium within the range $p=3\pm1$ per cent, $\phi=20\pm10°$, of IRS 1 and 5 are within 15° of those at 12.5 μm but that of IRS 10 does appear to be significantly different. There are other reasons, however, for supposing that the hot grains (~1000 K, Bailey *et al.* 1984) will be aligned differently from the cooler grains, and these are discussed in the next section.

Table 4. 3.5 μm polarization percentage and position angle.

	Observed		Intrinsic*	
	p	θ	p	θ
IRS 1	3.2	98 (1)	6.1	104
IRS 2	2.4	18 (2)	0.6	–
IRS 3	3.4	16 (1)	0.6	–
IRS 5	4.4	74 (1)	6.0	92
IRS 9	4.7	18 (1)	1.7	14
IRS 10	4.4	163 (3)	4.6	143

1. Averaged values from LRDK and KC.
2. KC.
3. LDRK.

*Intrinsic polarization found taking interstellar polarization of 3 per cent at position angle 20°.

4 The grain alignment mechanism in the Galactic Centre

We concern ourselves here only with the alignment mechanism of grains within the sources, and in particular with that producing the strongly polarized emission from the northern arc of sources. Here the polarization has all the characteristics of thermal radiation from aligned silicate grains. The alignment of grains in the interstellar medium, which produces the absorptive component, has been the subject of much discussion in the literature; we refer the reader to some of the many reviews of interstellar polarization (e.g. Purcell & Spitzer 1971; Purcell 1979; Johnson 1982).

Although the nature of the infrared sources in the Galactic Centre is still not clear, the physical condition and environment of the dust grains are reasonably well defined. The 10 μm discrete sources contain ionized gas with density $N_H \sim 10^5$ cm^{-3}, at temperature $T_{gas} \sim 10^4$ K. Each clump has dimension ~ 0.1 pc and probably contains $\sim 0.1\, M_\odot$ of gas. Radiation balance presumably controls grain temperatures but heating is only partly provided by resonant Lyman and other nebular radiation, and the bulk of the dust luminosity of $\sim 10^5\, L_\odot$ of each clump is presumably due to UV continuum radiation. The radiation field is relatively soft for the total luminosity and the 10 μm sources must be very optically thin on account of their resolved size and colour temperature.

In the Gold (1952) streaming mechanism for grain alignment the angular momenta of the grains become aligned in the plane normal to the direction of streaming; grains will then preferentially radiate with E-vector parallel to the streaming direction. LRDK have proposed that the grains in the Galactic Centre sources are aligned by streaming driven by radiation from UV sources embedded in the 10 μm sources, and point out that net polarization can only arise if the grain distribution about the sources is non-spherical. An immediate problem arises because of the large intrinsic polarization $\simeq 7$ per cent. This is discussed below.

Oblate grains are more efficient polarizers than prolate and an ensemble of oblate grains of axial ratio 2 and completely aligned with axis of symmetry in the plane of the sky would yield emission polarization $\simeq 35$ per cent (e.g. Lee & Draine 1985). In the limit of flat discs this increases by less than a factor 2 and as there is likely to be a distribution over a wide range of grain shapes, 35 per cent probably represents the maximum polarization ever to be expected from radiating grains. Streaming alignment can never give more than half this amount because the angular momentum axes are randomly distributed in a plane. An efficient way to provide net polarization by the streaming mechanism is to embed each source in a flat disc of material. A maximum polarization of 9 per cent then results if the grains are perfectly aligned by radial streaming and if the disc axis lies in the plane of the sky. At least 80 per cent of the observed emission would have to arise from such a disc whose axis of symmetry must lie along the line of the arc of sources. There is no sign of such a structure in any of the sources, although these are spatially well resolved at 10 μm. On the scale of the apertures used, the observed dust distribution is in a sense to produce polarization directed along the line of arc rather than normal to it if alignment were due to this mechanism. Similar arguments can be applied to the effects of a non-spherical radiation field due to the series of sources envisaged along the arc. Here streaming would be reduced between the sources and be greatest normal to the line of the arc. Polarization and its position angle would be a strong function of position along the arc and again more than 80 per cent of the emission would have to arise from grains which are completely aligned by the cylindrical component of radiation. As the bulk of the emission arises on a scale small compared with the spacing of the sources and therefore in a spherically symmetric radiation field, there would be no net alignment. We conclude that radiation driven streaming from internal sources is unable to account for the grain alignment in the northern arc. We can also rule out streaming alignment due to a central source of luminosity or a high velocity wind proposed to arise near the near infrared source IRS 16 (close to the non-thermal radio source SgrA*), because although

larger alignment can be achieved from directional streaming, there is no tendency for the position angles to be associated with IRS 16, roughly midway between IRS 1 and 2.

The correlation of polarization position angle with the normal to the line of the arc and the uniform and large polarization in the sources suggests a mechanism which directly reflects the morphology of the region. The most obvious candidate is, of course, a magnetic field directed along the line of the arc; as LRDK remark, this has to be very strong (>10 mG) to produce alignment in these dense regions.

The basic requirement of magnetic alignment is a large difference between the grain internal and rotational temperatures, and we need to establish that this can exist for the grains in the Galactic Centre. The internal temperature is ~200 K as indicated by the emission spectra and by photometry between 5 and 20 μm. In the absence of other effects the rotational temperature will be determined by collisions in the ionized gas, and will approach the gas temperature, $T_{\rm gas}\sim 10^4$ K, in a time

$$t_{\rm gas}=0.8\,\varrho a(3\,kT_{\rm gas}M_{\rm H})^{-1/2}/N_{\rm H}$$

(e.g. Martin 1978). In the conditions thought to prevail in the 10 μm sources, and for grains of radius $a\sim 10^{-5}$ cm and density $\varrho\simeq 2\,{\rm g\,cm^{-3}}$, then $t_{\rm gas}\sim 2$ yr. At these grain temperatures the possibility of the Purcell (1979) pinwheel mechanism operating through hydrogen recombination on grain surfaces seems unlikely, but other processes such as photoelectric emission from localized areas may be important. The grains also emit infrared photons copiously and each of these has intrinsic angular momentum, $h/2\pi$. The angular momentum transfer between the grains and their radiation field is a diffusive process which in effect introduces radiation damping; in the absence of other processes the rotational temperature will become less than the internal temperature and tend to $\sim T_{\rm grain}/2$ (Martin 1972; Purcell & Spitzer 1971).

To estimate the damping time due to thermal emission of photons we follow Harwit (1970). The rotational quantum number, J, for grains with rotational temperature $T_{\rm rot}$ and principal moment of inertia I will be

$$J\simeq 2\pi(IkT_{\rm rot})^{1/2}/h$$

while the probability of a decrease of J by unity per second is

$$N_{\rm n}\{{\rm Prob}(-)-{\rm Prob}(+)\}$$

where N_ν is the thermal emission rate of photons. Considering the grains to emit through vibration–rotation transitions,

$${\rm Prob}(-)-{\rm Prob}(+)\simeq 3\Delta\nu/\nu$$

(e.g. Herzberg 1950), and

$$t_{\rm rad}=J/[N_\nu\{{\rm Prob}(-)-{\rm Prob}(+)\}]\simeq \nu J/(3N_\nu\Delta\nu)$$

where

$$\Delta\nu\simeq(kT_{\rm rot}/I)^{1/2}/2\pi$$

is the contribution from rotational change. ν refers to the infrared emission from the grain and $\nu\sim kT_{\rm grain}/h$. Then,

$$t_{\rm rad}=32\pi^3a^5\varrho kT_{\rm grain}/(45h^2N_\nu)$$
$$\simeq 1.4\times 10^{38}a^5T_{\rm grain}/N_\nu$$

taking I to be the moment of inertia of a sphere of radius a and density $\varrho\simeq 2\,{\rm g\,cm^{-3}}$. N_ν depends on

the grain temperature, radius and absorption efficiency, and by integration of Planck functions,

$$N_\nu = 2.3\times10^{13}\, a^3 (T_{\rm grain})^4 \qquad \text{for } Q = 2\pi a/\lambda$$

or

$$= 3.8\times10^{14}\, a^4 (T_{\rm grain})^5 \qquad \text{for } Q = (2\pi a/\lambda)^2,$$

where Q is the absorption efficiency of the grains. The latter case applies to cold grains, such as in the interstellar medium, since in the limit of $a \ll \gamma$, $Q \sim (2\pi a/\lambda)^2$ (Purcell 1969b); $Q = 2\pi a/\lambda$ probably represents a maximum rate of emission for warm, small grains. Using these we find

$$t_{\rm rad} = 6.0\times10^{24}\, a^2 (T_{\rm grain})^{-3} \qquad \text{for } Q = 2\pi a/\lambda$$

or

$$= 3.7\times10^{23}\, a (T_{\rm grain})^{-4} \qquad \text{for } Q = (2\pi a/\lambda)^2.$$

For $a = 10^{-5}$ cm and $T_{\rm grain} \sim 200$ K, $t_{\rm rad}$ in these two cases is ~ 2.5 and 75 yr; for $T_{\rm grain} = 300$ K the corresponding times are ~ 0.7 and 15 yr. Alternatively using values of Q from Draine & Lee (1984) for silicate grains we find intermediate corresponding times of 20 and 6 yr for the two temperatures considered. We then estimate the grain rotational temperature from

$$T_{\rm rot} \simeq (T_{\rm grain}/2t_{\rm rad} + T_{\rm gas}/t_{\rm gas})/(1/t_{\rm rad} + 1/t_{\rm gas})$$

and provided $N_{\rm H} > 10^4$ cm^{-3} find that $T_{\rm rot}$ will be significantly greater than $T_{\rm grain}$. For warm grains, then, magnetic alignment can take place in dense ionized regions and requires magnetic fields large enough to make $t_{\rm mag}$ smaller than the other time constants of grain motion. For paramagnetic grains

$$t_{\rm mag} = 1.6\times10^{11}\, a^2 \varrho T_{\rm grain}/B^2$$

(e.g. Spitzer 1978), and for $t_{\rm mag} < t_{\rm gas}$, $B > 10^{-2}$ G. Such a large field within and directed along the arc is necessary to align these grains and would naturally account for the run of position angles.

It remains only to establish if under these conditions the intrinsic polarization of 7 per cent can be reasonably achieved. Following Greenberg (1968) we define an alignment parameter

$$R = \{3\langle \cos^2 \phi \rangle - 1\}/2$$

where ϕ is the angle between the angular momentum axis of the grains and the magnetic field and $\langle\ \rangle$ denotes the mean. R varies from 0 for no alignment to 1 for complete polar alignment (along the field direction) and $-1/2$ for complete equatorial alignment. For oblate grains of axial ratio 2 the maximum polarization fraction is 0.35, as discussed above, and $R > 0.07/0.35 = 0.2$. Purcell (1969a) gives a relation between the grain temperatures $T_{\rm grain}$ and $T_{\rm rot}$ and the value of R that can be produced by magnetic alignment. This shows that $R > 0.2$ for $T_{\rm grain} \simeq 200$ K and $T_{\rm rot} > 500$ K; R approaches a value of 0.6 if $T_{\rm rot} = T_{\rm gas} = 5000$ K (Brown & Liszt 1984). Thus the required alignments are feasible.

Because of the randomizing effects of thermal emission, the hot grains which emit at 3.5 μm can only be aligned in this way if $B > 0.2$ G and the gas density is larger by a factor ~ 100. If the gas is more compressed we may expect larger fields and perhaps that the position angle correlation becomes weaker. For adequate alignment with $T_{\rm grain} \sim 1000$ K, $T_{\rm rot}$ needs to be > 5000 K, which is as large as can be achieved by random processes in the gas. This problem, and to some extent the need for large densities, is reduced if photoelectric emission from grains has preferred sites which could lead to spin up. The process would be most effective near a source of UV photons but of course still requires this large magnetic field to align the spinning grains in a time $t_{\rm rad}$. The presence of significant 3.5 μm polarization lends weight to arguments that IRS 1, 5, and 10 contain their own luminosity sources.

The 8–13 μm spectropolarimetry also shows different polarization properties of the sources in the northern arc (1–10–5–8) and the bar (4–9–R–2–6). In the latter the intrinsic polarizations are systematically smaller, the spectra are less characteristic of intrinsic polarization (with consequently less evidence for emission from aligned grains), and the position angle correlations are weaker. These distinctions could all be reconciled with a field direction close to the line-of-sight, but Brown & Liszt (1984) have drawn attention to other physical dissimilarities between these two sequences. They refer to the northern arc (1–10–5–8) as part of a ring of ionized gas, whose extent is more completely delineated at radio frequencies, and the line (4–9–R–2–6) as the 'bar'. The arc, or ring, sources have gas temperatures ~5000 K, show a systematic trend of line-of-sight motion with relatively small velocity dispersion (36 ± 10 km s^{-1}; Serabyn & Lacy 1985), while sources in the bar have $T_{\rm gas}>12\,000$ K, very wide and structured line profiles (~200–400 km s^{-1}) and show a range of velocities along the bar with a discontinuity between IRS 1 and 2. The polarization data further emphasize the difference between these regions, and reveal the presence of a strong magnetic field which links the arc sources. In the bar the evidence for this is much weaker; it may be that the magnetic field is weak or absent, or that it, and by implication the bar, are inclined at a large angle to the plane of the sky.

It has been suggested (Brown & Liszt 1984) that the ring of radio emission and associated 10 μm sources is the hot, ionized inner rim of the 2 pc ring of cool dust and gas which is revealed by its 60 μm dust continuum (Becklin, Gatley & Werner 1982), H_2 (Gatley *et al.* 1984) and [O I] emission (Genzel *et al.* 1983). If this is the case and the magnetic field permeates this larger ring, polarization of the 60 μm emission is likely so long as a mechanism operates to maintain $T_{\rm rot}$ different from $T_{\rm grain}$.

The large intrinsic polarization does not apparently continue far beyond IRS 1. The magnetic field must of course be continuous and thus either lacks emissive material or, more interestingly, its direction approaches the line-of-sight close to the region most commonly accepted as the dynamical centre. This region, close to the non-thermal radio source, deserves further spectropolarimetric study.

5 Implications and speculation

The strength of the magnetic field in the northern arc is such that its energy density $B^2/8\pi>4\times10^{-6}$ erg cm^{-3} is large, much greater than the thermal energy of the gas $3NkT/2\sim10^{-7}$ erg cm^{-3} and comparable with the kinetic energy of the mass motions within each clump, which are $\sim2\times10^{-6}$ erg cm^{-3}. Consequently the field must be important dynamically and will affect the structure and evolution of the arc.

The magnetic pressure, directed radially outward from the arc, will tend to be disruptive unless there are other containing forces. These forces may arise if the field has a helical component which could conceivably provide a constraint on the material within the arc. However, in this case it seems that other instabilities would be introduced; matters would be still further complicated by interaction with the high velocity wind which appears to originate from near the non-thermal radio source.

Other consequences follow from the presence of this strong magnetic field.

First, the material in the arc is unlikely to be due to mass loss from interior objects. If this were the case the mass loss would carry fields local to the objects and the observed correlation of position angles along the arc would be hard to understand. The data rather require a pre-existing magnetized plasma and mass loss from interior objects must be sufficiently weak that it is channelled by the field.

Secondly, if the broad helium and hydrogen lines (Geballe *et al.* 1984) seen near IRS 16 are interpreted as outflow rather than rotation, then this wind will not be able to penetrate the arc

(the gyro-radius of a proton with velocity 750 km s^{-1} indicated by the broad line emission near IRS 16 is $\sim 10^6$ cm), while the wind may well carry a field of its own. Such a wind will, however, exert an outward pressure $\sim 3\times10^{-7}$ dyn cm^{-2} of rather larger amount than the internal arc pressure, if the mass loss rate of the wind is $\sim 10^{-3}\,M_\odot\,\mathrm{yr}^{-1}$ (Gatley *et al.* 1984). The compression of material by the wind may even be the origin of the arc and its large magnetic field. In opposition to gravitational forces towards the central mass concentration $\sim 10^6\,M_\odot$, the wind pressure may lead to Rayleigh–Taylor instabilities, perhaps accounting for the density concentrations 1–10–5–8.

Thirdly, similar arguments apply to the ring of cool dust and gas. Weak ionization by cosmic rays will ensure flux freezing and only a very weak field would allow the wind access to the ring; shock excitation of molecular hydrogen (Gatley *et al.* 1984) must be indirect through coupling of mechanical energy via magnetic fields.

Fourthly, the presence of a magnetic field in the arc suggests that much larger fields may be present in regions close to a central object, and this would have consequences concerning the variable annihilation radiation (Matteson 1982; Jacobson 1982; Leventhal & MacCallum 1982; Paciesas *et al.* 1982). Lingenfelter & Ramaty (1982) point out that the high efficiency of positron production implied by the observed ratio of annihilation to γ continuum radiation places severe constraints on the positron production mechanism, and requires that it is confined to a very small region $\sim 5\times10^8$ cm with implied black hole mass $<500\,M_\odot$. Lingenfelter & Ramaty point out that these constraints would be relaxed if the γ-ray continuum is directed away from the line-of-sight and a large magnetic field could achieve this through synchrotron cooling. For example, in a relativistic gas of density 10^9 cm^{-3} synchrotron losses exceed ionization and bremsstrahlung losses in a field ~ 500 G unless electron velocities are within $\sim 10°$ of the field direction, thus collimating the bremsstrahlung in this direction and allowing much smaller positron production efficiencies. With this constraint relaxed other processes, such as particle–particle interactions, may contribute (Lingenfelter & Ramaty 1982, 1983) and a larger region of positron production than required by the isotropic photon–photon model becomes possible. Kardashev *et al.* (1983) have proposed a 'gamma-gun' at the Galactic Centre, also invoking strong local fields, to explain the various features of the annihilation radiation.

There has been a wide range of speculation regarding the inner structure of the Galaxy, from inflow of material along the E–W bar (Ekers *et al.* 1983) to outflow represented by the broad helium lines seen near SgrA* (Geballe *et al.* 1984), while the kinematics of the northern and western arcs suggest orbiting material inclined to the line-of-sight and rotating about a region near SgrA* (Serabyn & Lacy 1985). Recent theoretical modelling of the central parsec (Quinn & Sussman 1985) suggests that the arc of sources 1–10–5–8 is a tidally disrupted filament falling into the centre, whilst the E–W arm, or bar, may represent outflow from the core. Certainly the structures are observationally dissimilar on a number of counts and further spectropolarimetry will be of value. We plan higher spatial resolution spectropolarimetric studies of the region close to SgrA* and a more detailed study of the bar region in the near future.

6 Conclusions

Spectropolarimetry between 8 and 13 μm of Galactic Centre sources confirms the presence of interstellar and intrinsic components of polarization and provides further information on the distribution of interstellar matter along the line-of-sight, on the nature of the intrinsic polarization, and the grain alignment mechanism:

(1) The interstellar polarization at 10 μm is due to absorption by aligned grains of silicate-like material. Comparison of the 10 and 2 μm polarization amplitudes and position angles suggests

that the silicate and other components of grain material are fractionated along the line-of-sight, and that there is a larger proportion of silicate material than in Orion. This gives independent support to earlier independent evidence that the interstellar medium in the central regions of the Galaxy is enriched in silicate grains (RA).

(2) Intrinsic polarization is large and ~7 per cent in the northern arc of sources and appears to be due to thermal emission from aligned silicate grains. The degree of alignment of grains is stronger than in any source studied so far. The polarization spectrum indicates a material of relatively low bandstrength, typical of amorphous silicates.

(3) Alignment of dust grains by streaming cannot account for the strength or orientation of polarization in the nothern arc. Rather, the uniformity of polarization and the run of position angles indicate the presence of a strong magnetic field $>10^{-2}$ G directed along the arc and linking these sources. It is shown that, in a dense ionized region, the Davis–Greenstein mechanism can provide a sufficient degree of alignment of these warm grains to account for the observed polarization.

(4) The intrinsic polarization is much weaker in most of the sources in the E–W bar, although silicate emission is still evident. The physical conditions affecting alignment appear little different in these two structures and it seems that in the bar the magnetic field is either much weaker or inclined at a large angle to the plane of the sky.

(5) The strong magnetic field in the nothern arc will be important dynamically, and in spite of the complexity and intractability of the problem, a dynamical picture of the central region of the Galaxy will be incomplete until the effects of magnetohydrodynamics are included. Qualitatively the most obvious effects of the field will be disruptive, giving further indication of the transient nature of the present configuration. More speculatively, the presence of a magnetic field suggests stronger centrally concentrated fields which could lead to collimation of high energy electromagnetic processes and a relaxing of constraints on the positron production mechanism.

Acknowledgments

We are grateful for the assistance of the staff of the Anglo-Australian Telescope, for the award of telescope time by ATAC and for useful discussions with Professor Opat of the School of Physics at Melbourne University. We also wish to thank an anonymous referee. This work was given financial support by the Australian Research Grants Scheme.

References

Aitken, D. K., Bailey, J. A., Briggs, G. P., Hough, J. H. & Roche, P. F., 1984. *Nature,* **310,** 660.
Aitken, D. K., Bailey, J. A., Roche, P. F. & Hough, J. H., 1985. *Mon. Not. R. astr. Soc.,* in press (ABRH).
Bailey, J., Hough, J. H. & Axon, D. J., 1984. *Mon. Not. R. astr. Soc.,* **206,** 661.
Becklin, E. E., Mathews, K., Neugebauer, G. & Willner, S. P., 1978. *Astrophys. J.,* **219,** 121.
Becklin, E. E., Gatley, I. & Werner, M. N., 1982. *Astrophys. J.,* **258,** 135.
Blanco, B. M., Blanco, V. M. & McCarthy, M. F., 978. *Nature,* **271,** 638.
Brown, R. L. & Liszt, H. S., 1984. *A. Rev. Astr. Astrophys.,* **22,** 223.
Capps, R. W. & Knacke, R. F., 1976. *Astrophys. J.,* **270,** 76.
Davis, L. & Greenstein, J. L., 1951. *Astrophys. J.,* **114,** 206.
Draine, B. T. & Lee, H. M., 1984. *Astrophys. J.,* **285,** 89.
Dyck, H. M., Capps, R. W. & Beichman, C. A., 1974. *Astrophys. J.,* **188,** L103.
Dyck, H. M. & Lonsdale, C. J., 1981. *IAU Symp. No. 96, Infrared Astronomy,* p. 223, eds Wynn-Williams, C. G. & Cruikshank, D. P., Reidel, Dordrecht.
Ekers, R. D., van Gorkom, J. H., Schwarz, U. J. & Goss, W. M., 1983. *Astrophys. J.,* **122,** 143.
Gatley, I., Hyland, A. R., Jones, T. J., Beattie, D. H. & Lee, T. J., 1984. *Mon. Not. R. astr. Soc.,* **210,** 565.
Geballe, T. R., Krisciunas, K., Lee, T. J., Gatley, I., Wade, R., Duncan, W. D., Garden, R. & Declin, E. E., 1984. *Astrophys. J.,* **284,** 118.

Genzel, R., Watson, D. M., Townes, C. H., Dinerstein, H. L., Hollenbach, D., Lester, D. F., Werner, M. & Storey, J. W. V., 1984. *Astrophys. J.,* **276,** 551.
Gold, T., 1952. *Mon. Not. R. astr. Soc.,* **112,** 215.
Greenberg, J. M., 1968. *Nebulae and Interstellar Matter*, p. 221, eds Middlehurst, B. M. & Aller, L. H., University of Chicago Press.
Harwit, M., 1970. *Bull. astr. inst. Czech.,* **21,** 204.
Heckert, P. A. & Zeilik, II, M., 1984. *Astr. J.,* **89,** 1379.
Herzberg, G., 1950. *Spectra of Diatomic Molecules*, p. 126, van Nostrand.
Hong, M. & Greenberg, J. M., 1978. *Astr. Astrophys.,* **70,** 695.
Jacobson, A. S., 1982. *AIP Conference Proceedings No. 83, The Galactic Centre*, p. 123, eds Riegler. G. R. & Blandford, R. L., American Institute of Physics, New York.
Johnson, P. E., 1982. *Nature,* **295,** 371.
Kardashev, N. S., Novikov, I. D., Ponarev, A. G. & Stern, B. E., 1983. *AIP Conference Proceedings No. 101, Positron–Electron Pairs in Astrophysics*, p. 253, eds Burn, M. L., Harding, A. K. & Ramaty, R., American Institute of Physics, New York.
Kobayashi, Y., Kawara, K., Kozasa, T., Sato, S. & Okuda, H., 1980. *Pub. astr. Soc. Jap.,* **32,** 291.
Kobayashi, Y., Okuda, H., Sato, S., Jugaku, J. & Dycke, H. M., 1983. *Pub. astr. Soc. Jap.,* **35,** 101.
Knacke, R. F. & Capps, R. W., 1977. *Astrophys. J.,* **216,** 271 (KC).
Lacy, J. H., Townes, C. H., Geballe, T. R. & Hollenbach, D. J., 1980. *Astrophys. J.,* **241,** 132.
Lebofsky, M. J., Rieke, G. H., Deshpande, M. R. & Kemp, J. C., 1982. *Astrophys. J.,* **263,** 672 (LRDK).
Lee, H. M. & Draine, B. T., 1985. *Astrophys. J.,* **290,** 211.
Leventhal, M. & MacCallum, C. J., 1982. *AIP Conference Proceedings No. 83, The Galactic Centre*, p. 132, eds Riegler, G. R. & Blandford, R. L., American Institute of Physics, New York.
Lingenfelter, R. E. & Ramaty, R., 1982. *AIP Conference Proceedings No. 83, The Galactic Center*, p. 148, eds Riegler, G. R. & Blandford, R. L., American Institute of Physics, New York.
Lingenfelter, R. E. & Ramaty, R., 1983. *AIP Conference Proceedings No. 101, Positron–Electron Pairs in Astrophysics*, p. 267, eds Burns, M. L., Harding, A. K., & Ramaty, R., American Institute of Physics, New York.
Lo, K. Y. & Claussen, M. J., 1983. *Nature,* **306,** 647.
Martin, P. G., 1972. *Mon. Not. R. astr. Soc.,* **158,** 63.
Martin, P. G., 1975. *Astrophys. J.,* **202,** 393.
Martin, P. G., 1978. *Cosmic Dust*, Oxford.
Matteson, J. L., 1982. *AIP Conference Proceedings No. 83, The Galactic Centre,* p. 109, eds Riegler, G. R. & Blandford, R. L., American Institute of Physics, New York.
Paciesas, W. S., Cline, T. L., Teegarden, B. J., Tuellewr, J., Durouchoux, P. & Hameury, J. M., 1982. *AIP Conference Proceedings No. 83, The Galactic Centre,* p. 139, eds Riegler, G. R. & Blandford, R. L., American Institute of Physics, New York.
Purcell, E. M., 1969a. *Physica,* **41,** 100.
Purcell, E. M., 1969b. *Astrophys. J.,* **158,** 433.
Purcell, E. M., 1979. *Astrophys. J.,* **231,** 404.
Purcell, E. M. & Spitzer, L., 1971. *Astrophys. J.,* **167,** 31.
Quinn, P. J. & Sussman, G. J., 1985. *Astrophys. J.,* **288,** 377.
Roche, P. F. & Aitken, D. K., 1984. *Mon. Not. R. astr. Soc.,* **209,** 35P.
Roche, P. F. & Aitken, D. K., 1985. *Mon. Not. R. astr. Soc.,* in press.
Russell, R. W., Soifer, B. T. & Forrest, W. J., 1975. *Astrophys. J.,* **198,** L41.
Serabyn, E. & Lacy, J. H., 1985. *Astrophys. J.,* **293,** 445.
Serkowski, K., 1962. *Adv. Astr. Astrophys.,* **1,** 289.
Spitzer, L., 1978. *Physical Processes in the Interstellar Medium,* p. 184, John Wiley & Sons.
Wardle, J. F. C. & Kronberg, P. P., 1974. *Astrophys. J.,* **194,** 249.
Wilking, B. A., Lebofsky, M. J., Martin, P. G., Rieke, G. H. & Kemp, J. C., 1980. *Astrophys. J.,* **235,** 905.